INT. J. REMOTE SENSING, 2000, VOL. 21, NO. 6 & 7, 1115–1138

Application of the MODIS global supervised classification model to vegetation and land cover mapping of Central America

D. MUCHONEY†, J. BORAK, H. CHI, M. FRIEDL, S. GOPAL, J. HODGES, N. MORROW and A. STRAHLER

Center for Remote Sensing, Department of Geography, Boston University, 675 Commonwealth Avenue, Boston, MA 02215, USA

Abstract. While mapping vegetation and land cover using remotely sensed data has a rich history of application at local scales, it is only recently that the capability has evolved to allow the application of classification models at regional, continental and global scales. The development of a comprehensive training, testing and validation site network for the globe to support supervised and unsupervised classification models is fraught with problems imposed by scale, bioclimatic representativeness of the sites, availability of ancillary map and high spatial resolution remote sensing data, landscape heterogeneity, and vegetation variability. The System for Terrestrial Ecosystem Parameterization (STEP)—a model for characterizing site biophysical, vegetation and landscape parameters to be used for algorithm training and testing and validation—has been developed to support supervised land cover mapping. This system was applied in Central America using two classification systems based on 428 sites. The results indicate that: (1) it is possible to generate site data efficiently at the regional scale; (2) implementation of a supervised model using artificial neural network and decision tree classification algorithms is feasible at the regional level with classification accuracies of 75–88%; and (3) the STEP site parameter model is effective for generating multiple classification systems and thus supporting the development of global surface biophysical parameters.

1. Introduction

Maps of the distribution and status of the Earth's vegetation and land cover are critical for both parameterization of global climate and ecosystem process models and characterization of the distribution and status of major land surface types for environmental, ecological and natural resource applications at global and meso-scale levels. The distribution of land surface parameters that are related to climate must be prescribed as inputs to global models (Henderson-Sellers 1987). These land surface biophysical parameters are closely linked to classification systems as applied to remotely sensed data, while mapped classifications are reliant on some level of site-based characterization of surface and vegetation attributes for algorithm training, testing and map product validation. The current approach to defining surface parameters in the absence of field-derived parameters is to use land cover, vegetation or land surface classification schemes. These schemes are generally derived from remote sensing data of reflectance, radiance and the Normalized Difference Vegetation Index

†E-mail address: muchoney@bu.edu. Tel: 617 353 1049. Fax: 617 353 3200.

International Journal of Remote Sensing
ISSN 0143-1161 print/ISSN 1366-5901 online © 2000 Taylor & Francis Ltd
http://www.tandf.co.uk/journals/tf/01431161.html

(NDVI), and specify the relationship between the remote sensing observation and derived land surface parameters (Sellers *et al.* 1996). In the context of regional conservation and resource management, detailed maps of land cover, vegetation and ecosystems derived from remotely sensed data are needed.

1.1. *Regional and global land cover characterization*

While there is a tremendous history of mapping, validation and generation of reliable surface parameters based on mapping and field inventory at the local scale, such as those derived by Sellers *et al.* (1989) for the Amazon tropical forest biome, sheer size has precluded the development of training and test site data at regional, continental and global scales. Current mapping of land cover at regional and global scales has been based on National Oceanic and Atmospheric Administration Advanced Very High Resolution Radiometer (NOAA AVHRR) data. As early as 1985, Tucker *et al.* developed a land cover map of Africa and Townshend *et al.* (1987) created a map of South America based on multi-temporal AVHRR Global Area Coverage (GAC) data. The land cover of Stone *et al.* (1994) for South America was developed from multiple sources and resolutions of thematic maps and remote sensing data. There are now numerous other studies that have applied land cover systems regionally based on AVHRR data, for example those of Malingreau (1986) and Achard and Estreguil (1995).

Loveland *et al.* (1991, 1995) produced land cover maps using the International Geosphere–Biosphere Program (IGBP) classification and Seasonal Land Cover Region (SLCR) classification systems for North America. These efforts were later expanded to be the first global map of land cover based on 1 km multi-temporal AVHRR Local Area Coverage (LAC) data (Belward and Loveland 1995). Global land cover at a 1-degree resolution for 11 land cover classes has been achieved by DeFries and Townshend (1994), Friedl and Brodley (1997), Friedl *et al.* (1999) and Gopal *et al.* (1999). Other global maps and databases of land cover that have been used to estimate and infer surface parameters include those of Matthews (1983), Olson and co-workers (Olson and Watts 1982, Olson *et al.* 1983) and Wilson and Hendersen-Sellers (1985).

The 1 degree AVHRR analyses of DeFries and Townshend (1994), Friedl and Brodley (1997), Friedl *et al.* (1999) and Gopal *et al.* (1999) are based on the agreement of the maps of Matthews (1983), Olson and co-workers (Olson and Watts 1982, Olson *et al.* 1983) and Wilson and Hendersen-Sellers (1985) to define training and test data. While the global land cover of Loveland *et al.* (1995) is derived using an unsupervised approach and is currently being validated, only the 1 degree and 8 km maps of DeFries and Townshend (1994) have been based on site data for training and validation. In this instance, training and test site data were based on delineating polygons on Landsat Multispectral Scanner (MSS) and Thematic Mapper (TM) data and assigning them 11 categorical land cover labels. Site generation for classification and mapping purposes has been somewhat *ad hoc*, and there has been no formal global database strategy developed to support continuous generation of map products that are scheduled to be produced from Moderate Resolution Imaging Spectroradiometer (MODIS) data (Justice *et al.* 1998).

1.2. *MODIS 1 km land cover and land cover change*

The primary purpose of MODIS land cover characterization (Strahler *et al.* 1996) is to support global modelling either indirectly by providing inputs to MODIS

algorithms that generate parameters including leaf area index/fraction of photosynthetically active radiation (LAI/FPAR), the bidirectional distribution function (BRDF), vegetation indexes (VI) and surface temperature or directly as land cover inputs to models. User-operated models then may translate the remote sensing derived land cover to a model-specific classification scheme and obtain needed parameters using look-up tables.

Boston University will produce global land cover and land cover change products globally at 1000 m and 0.25 degree resolutions quarter-annually using an annual temporal sequence of multispectral and multi-resolution MODIS data as part of the NASA-supported Earth Observing System (EOS) MODIS program. The principal inputs to the quarterly land cover products are monthly BRDF, BRDF-corrected nadir surface reflectances, vegetation index, snow cover, land surface temperature and spatial texture for a one-year sequence (Strahler *et al.* 1996). Several types of decision tree (DT) and artificial neural network (ANN) classification algorithms are currently being evaluated for their utility for generating the global MODIS 1 km land cover product. The DT algorithms include univariate DTs (e.g. Quinlan 1993), multivariate DTs (Brodley and Utgoff 1995) and hybrid trees Brodley (1995). The neural network (NN) algorithms that are being tested include the Fuzzy-ARTMAP (Carpenter *et al.* 1991a, b, 1992) and Gaussian ARTMAP (Williamson *et al.* 1995) algorithms.

Evaluation of these different NN and DT classification algorithms using several remote sensing data sets has shown that these algorithms produce comparable results that are consistently superior to those produced by maximum likelihood classification (Gopal *et al.* 1999, Friedl and Brodley 1997). The final classification algorithm will therefore be either a univariate DT based on the C4.5 algorithm (Quinlan 1993), supervised NN (Gopal *et al.* 1994, 1999), or a hybrid of these two classification models**.** While the primary system of land cover classification to be employed is the 17-class IGBP classification (Belward and Loveland 1995), a functional and efficient training and test site characterization approach must support other classification systems, and allow for direct estimation and inference of surface parameters.

1.3. *Objectives*

The purpose of this paper is to describe recent research in the development and application of a supervised classification approach to global land cover mapping that will be based on MODIS data. This experience results from the development of a training, testing and validation model and database, the System for Terrestrial Ecosystem Parameterization (STEP), and its application in Central America to mapping multiple land cover and vegetation classification systems and parameters using artificial NN and DT algorithms.

A major objective and component of this effort to characterize the regional vegetation and land cover of Central America is to expand rapid ecological assessment (REA) (Muchoney *et al.* 1991) approaches to using remote sensing data to support vegetation and ecosystem characterization from the site and macrosite level to the regional level. The mapping and description of the vegetation and land cover of Central America developed for this study employs multistage sampling based on remote sensing at both the site and regional levels. Current characterizations of the vegetation and land cover are needed to support biodiversity conservation and management of protected areas, especially the development of the Meso-American Biodiversity Corridor. A parallel objective is to develop and test a methodology for

supervised classification that can be implemented globally using MODIS data, hence the need to apply multiple land cover classification systems simultaneously.

This paper describes the generation of a classification system and map from a plot-based land surface parameter database for Central America. The analysis employed multi-temporal NOAA-AVHRR satellite data, and plot/site data obtained through feature extraction at 428 sites based on Landsat TM, Satellite pour l'Observation de la Terre (SPOT), AVHRR, and existing vegetation and land cover data. These data were used to apply supervised classifications based on ANN, DT and maximum-likelihood classification algorithms. This study produced (1) a new classification system of vegetation and land cover; (2) maps of the vegetation and land cover and IGBP systems based on supervised classification of the AVHRR and ancillary data; and (3) a site parameter database for Central America.

2. Site and data

2.1. *Site*

The dimensions of the study area are 1169×1813 1 km AVHRR pixels, bounded by 6° to 9° north latitude and 77.22° to 93° west longitude (figure 1). The study area comprises southern Mexico, Guatemala, Belize, Honduras, El Salvador, Nicaragua, Costa Rica and Panama. Central America includes a diverse array of natural and human-modified landscapes including broadleaf evergreen, deciduous and semi-deciduous forests, pine savanna and woodlands, swamp and mangrove forests, herbaceous wetlands, and agriculture.

2.2. *Remotely sensed data*

The primary remotely sensed data used in this study were monthly composited AVHRR NDVI data provided by the US Geological Survey EROS Data Center

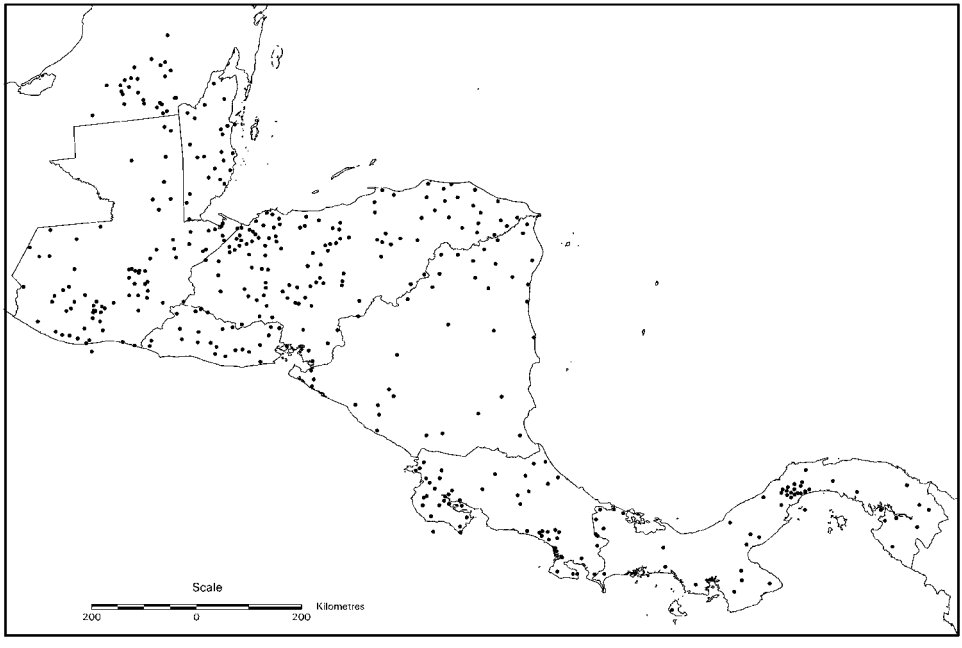

Figure 1. Site distribution map.

(USGS-EDC) (Eidenshink and Faundeen 1994), in lieu of MODIS data which will be used for generating global 1 km land cover following its launch on the EOS-AM platform in 1999. The NDVI is based on the relationship of reflected red and near-infrared reflectance which is highly correlated with both LAI and biomass. The monthly data provide an indication of overall greenness of the vegetation, and can be used to characterize the phenology of vegetation. The AVHRR data were monthly composited using maximum NDVI values to remove cloud and topographic effects and extreme off-nadir pixels (Holben 1986, Eidenshink and Faundeen 1994), as well as scan angle dependence of radiance (Duggin *et al.* 1982).

The use of the monthly-composited AVHRR data may be problematic (Holben 1986). An analysis by Zhu and Yang (1996) determined that compositing was biased towards selecting off-nadir pixels, especially in forward-scanning views in winter months in the Northern Hemisphere. As with any large-area projection, they also found that the effective mapping unit was geographically variable, in this case due to Goode's homolosine projection system and resampling methods (Zhu andYang 1996). Lack of sensor calibration confuses the temporal trajectory of the multi-temporal NDVI signal (Cihlar 1996). Temporal smoothing or generalization might enhance the meaning of the temporal signal (Van Dijk *et al.* 1987), but this technique was not applied to the data set used in this study.

While 1 km AVHRR NDVI data lack the spectral resolution, radiometric calibration and locational accuracy qualities of MODIS data, they do provide a regional, multi-temporal dataset, and maximum value NDVI monthly compositing removed many of the atmospheric effects evident in the daily or 10-day composite data for the same period. A land/sea mask was applied to the AVHRR data as part of the processing. In some cases, such as in the region of Mosquitia in Honduras and Nicaragua, there was not a good coincidence with the actual coastline based on comparison with geo-coded TM data. This problem, however, does not significantly impact the analysis as water-contaminated sites were screened from the operational site database.

2.3. *The STEP model and site database*

To meet the requirements for multivariable site model and database for training, testing and validation, the STEP was developed. STEP is a multivariable site database framework for describing site vegetation, environment and other biophysical parameters (Muchoney *et al.* 1999). STEP is a formal model that relates multisource remote sensing, field and thematic data to landscape biogeophysical attributes to permit training, testing, parameterization and validation. It provides for continuous acquisition and update of plot-level data that can be applied to classification algorithm training, testing and validation, as well as to more comprehensive ecological/environmental description. It is a classification-free approach that is appropriate at multiple scales and for multiple landscape classifications that utilize physiognomic, functional, structural and phenologic criteria. The STEP allows for training and testing of classification algorithms, and validating map product accuracy.

STEP is being used to create a global database of land cover test sites and associated parameters which can also be applied to direct generation of multiple classification systems and specific biophysical parameters. Feature extraction and parameterizing the STEP database involves assigning labels to appropriate categories of a suite of parameters. STEP provides explicit descriptions of the structural, functional and compositional components of the vegetation and landscape tied to specific sites and plots

(table 1). Its primary purpose is to provide a comprehensive model of the land surface that can be used to train and test algorithms and to validate land surface products. Formal sites are established and described based on high resolution remote sensing, ancillary and field plot data. STEP can be used to translate multiple classification systems as an alternative to commonly used look-up table approaches. This accommodates the wide array of classifications used by various models to parameterize biophysical processes such as those of Biosphere–Atmosphere Transfer Scheme (BATS) (Dickinson *et al*. 1993), Biome-BGC (Running *et al*. 1994, 1995, Nemani and Running 1996, 1997, Myneni *et al*. 1997), the Land Surface Model (LSM) (Bonan 1996) and Simple Biosphere models (SiB, Sellers *et al*. 1986; SiB2, Sellers *et al*. 1996).

Table 1. STEP site parameters.

Vegetation parameters
physiognomy
phenology
periodicity
horizontal structure: cover fraction at each strata for two seasons, distribution
vertical structure: strata, strata height
canopy: base height, height, cover fraction for two seasons
canopy radiative properties
Leaf parameters
morphology
LAI
LAD
leaf photosynthetic surface
Optical properties
leaf optical properties
reflectance
bidirectional reflectance
VI
texture
Physical site and landscape parameters
elevation
slope aspect
slope angle
location
continentality
patch perimeter
patch area
snow cover
surface temperature
Soil and hydrologic parameters
soil type
soil moisture
soil texture
soil color
hydrologic regime
***A priori* classification systems**
global ecosystems (Boston University)
IGBP
physiognomic-structural (Boston University)

2.4. *Classification systems*

For Central America, there are a number of classification systems that have been developed for local and country-wide use; only a small number has been applied to the whole of Central America, and even fewer applied using current remote sensing data. Remote sensing based maps include those produced for the IGBP (Belward and Loveland 1995, Loveland *et al.* 1995) and the land cover map of Stone *et al.* (1994). Maps not based on remote sensing but on climate and other data include the terrestrial ecoregions of Dinerstein *et al.* (1995) and the maps of Diego-Gomez (1985). The bio-climatic Holdridge Life Zone System (Holdridge 1967) is also employed widely throughout the region (Holdridge 1962 a,b, 1975a, b).

The STEP database includes attributes for several classification systems that can either be directly attributed to a site, or derived from more basic site data on physiognomy, structure, site and floristics. These classification systems include the IGBP system, which was used in this study. In addition to IGBP, a new Vegetation and Land Cover (VLC) classification system was developed by a working group for application to the region to support the development of a Meso-American biodiversity corridor. VLC is intended to be used with multi-temporal 1 km AVHRR data and, ultimately, MODIS data. It is primarily related to vegetation physiognomy, phenology, periodicity, morphology, and horizontal and vertical structure.

2.5. *Site database development*

The data for training and testing the supervised classification algorithms were developed by Boston University, the Stanford University Center for Conservation Biology, The Nature Conservancy and the Central America Vegetation Working Group which was established to support vegetation mapping and monitoring in Central America. The Working Group comprised two vegetation experts for each country in the study area. Pairs of analysts delineated sites on TM, SPOT and AVHRR data, and populated the database based on field, plot and ancillary map data at two workshops held in Guatemala and Nicaragua.

A total of 450 sites were distributed among the 25 VLC classes and extracted from 18 TM and 2 SPOT scenes (figure 1). The criteria used for site selection were that the site must be at least 2 km $\times$ 2 km in area and regionally representative of the VLC classes. The site polygons were also defined to be within larger patches of classes, with at least a 1 km buffer from the polygon boundary to the patch boundary. This was to ensure that misregistration and mislocation of the AVHRR data and the co-referenced TM or SPOT data would not permit a training polygon to actually represent land cover outside of the patch. After a quality assurance check was performed to ensure that the site data labels were correct, 22 sites were removed from the database because they were either obviously mislabelled or did not meet the minimum site size criteria.

From the remaining 428 sites, subsets of train (80%) and test (20%) pixels were randomly generated by random sampling to allow for independent training and accuracy assessment. In this approach, the algorithm trains on 80% of the total site pixels, and its accuracy is assessed for the remaining 20% of pixels, which are unseen. Since results are sometimes dependent on the actual random selection of pixels, the subsampling procedure was repeated five times, thus providing five sets of training and testing pixels to the classification and accuracy assessment process. The use of the 80/20 train to test ratio was based on the need to provide as many training data

examples to the classification algorithms, and its appropriateness was confirmed by empirical testing of other train to test ratios.

3. Analytical approach

Four supervised classification algorithms, comprising two artificial NNs, a univariate DT and a maximum-likelihood Bayesian (MLC) classification algorithm were applied to the classification of the AVHRR data. Both the ANN and DT algorithms have been shown to be improvements over traditional maximum-likelihood decision rules based on their ability to partition data in nonlinear and non-parametric fashions (Gopal *et al.* 1994, 1996). The MLC algorithm was applied as a benchmark for the performance of the NN and DT classification algorithms.

Neural nets are complex and dense systems of nonlinear computational elements that are patterned after bio-neurological systems that are composed of computational nodes linked by adaptive weights (Lippmann 1989). The neural nets used in this analysis are from the class of Adaptive Resonance Theory (ART) (Carpenter *et al.* 1991 a) networks, including Fuzzy ARTMAP (Carpenter *et al.* 1991 b, 1992) and Gaussian ART (Williamson 1995). ART NNs process inputs into categories, with the category formation being governed by a set of parameters including a vigilance parameter (ρ) which regulates how broad a category might be, the choice function (α) which determines that category to which any input might belong, and the match function which determines if a selected category is sufficiently appropriate to meet the vigilance criteria (Williamson 1995). These categories are related to specific output classes in such a way that they represent multiple, nonlinear partitions of feature space that map to output classes.

Gaussian ARTMAP is a supervised (and unsupervised) NN based on ART that uses Gaussian-defined receptive fields. Its internal categories model a local density of the input space and map an output class prediction. Each category's receptive field is a Gaussian distribution parameterized by mean, standard deviation and scalar that represents the amount of training data for which each node has received credit (*a priori* probability). Gaussian ARTMAP, like maximum-likelihood, is based on the assumption that the input channels are normally distributed and that the training data statistics for each class, which can be thought of as samples, are also normally distributed. In a supervised mode, Gaussian ARTMAP chooses an output class with the maximum probability estimate for a given input. In an unsupervised mode, Gaussian ARTMAP distinguishes clusters based on Gaussian distributions in the input data.

Fuzzy ARTMAP uses a choice function (α) based on fuzzy logic, while for Gaussian ARTMAP the choice function (γ) is based on defining each ART category by one or more separable Gaussian distributions. The choice function picks the most likely prediction of a class based on this distribution. For both Fuzzy ARTMAP and Gaussian ARTMAP, inputs are generalized through unsupervised clustering first, while the vigilance (ρ) and match tracking parameters influence the generation of new categories and ultimately to what degree the classification algorithm generalizes or fits inputs to outputs. For Gaussian ARTMAP, high vigilance (ρ) means that more internal categories are created by the network to match input data to output categories; i.e. the categories are less broad. For Fuzzy ARTMAP, small choice parameter values (α) generate large categories in feature space, while high values of α promote the generation of small categories (Williamson 1995).

A DT is defined as a classification procedure that recursively partitions a data

set into more uniform subdivisions based on tests defined at each branch (or node) in the tree (see, for example, Quinlan 1993). A DT is composed of a root node (i.e. all of the data), a set of internal nodes (splits) and a set of terminal nodes (leaves). Each internal node in a DT has one parent node and two or more descendant nodes. Using this framework, a data set is classified according to the decision surfaces defined by the tree, and class labels are assigned to each observation according to the leaf node into which the observation falls.

Boosting is a recent technique developed in the machine learning community that has been shown to significantly improve the performance of DT classification algorithms (e.g. Quinlan 1996). The goal of boosting is to improve the classification accuracy of a given base classification algorithm (Shapire 1990). To do this, boosting algorithms estimate multiple classifications in an iterative fashion using the base classification algorithm (e.g. a DT). At each iteration, a weight is assigned to each training observation, where those observations that were misclassified in the previous iteration are assigned a heavier weight in the current iteration. This forces the classification algorithm to concentrate on those observations that are more difficult to classify. Friedl *et al.* (1999) have recently tested boosting using DTs to classify AVHRR data and have shown that boosting consistently improves classification results.

The MLC calculates the probability that a pixel belongs to one of the set of possible classes based on the mean measurement vector for each class and the covariance matrix for each class by band. The probability that a pixel belongs to a class is based on the distance between the pixel and a scaled and variance/covariance-corrected class mean (Strahler 1980). The pixel is then assigned to that class to which the weighted distance is the lowest. The principal assumptions of the MLC are that the input channels are Gaussian (normally) distributed and that the training data statistics for each class, which can be thought of as samples, are also normally distributed. It also assumes that the probabilities are equal for each class unless this assumption is modified by adjusting the prior probabilities.

3.1. *Supervised Vegetation and Land Cover classification*

The distinct classification system requirements of partner organizations allowed the testing of regional classification using both the IGBP and VLC classification systems. This provided the opportunity to test the classification algorithm performance and the utility of the STEP model and database for providing data to train, test and validate different classifications systems. First, supervised classification based on each of the five IGBP random train and test subset splits was performed using the Gaussian ARTMAP, Fuzzy ARTMAP, DT and MLC algorithms. This method allows for robust estimation of classification accuracy. Second, based on the results of this exercise, Gaussian ARTMAP was applied to the five sets of train and test data for the VLC system to map that classification system. All supervised algorithms were applied to the Central America STEP site data by training and testing on the monthly-composited NOAA AVHRR data for 12 months of 1992 and 1993 (Eidenshink and Faundeen 1994). The monthly data are the inputs to the various classification algorithms.

3.1.1. *Regional supervised IGBP classification*

The STEP IGBP labels for the five train and test splits of the 428 sites were applied to the Gaussian ARTMAP, Fuzzy ARTMAP, DT, and MLC algorithms.

For all approaches, the error rates were similar for all five of the train–test pixel splits (table 2). For the Fuzzy ARTMAP classification, the choice parameter α was applied thorough its range of 0.01–0.99 to determine the optimum value based on the classification accuracy of unseen test pixels. An α value of 0.95 was selected, and applied to the five train–test data splits. The mean overall accuracy for the Fuzzy ARTMAP runs is 79.30% . The mean accuracy of the DT applied without boosting was 74.79%, while boosting improved the mean accuracy to 88.16%.

The MLC algorithm was applied without prior probabilities (Strahler 1980). The mean overall accuracy of the MLC was poor in comparison to the other algorithms with accuracies ranging from approximately 49–53%. The mean accuracies of the five Gaussian ARTMAP iterations is 82.77%. An example contingency table taken from Gaussian ARTMAP run 1 is presented as table 3 to describe the per-class errors and inter-class confusion. As tables 2 and 3 indicate, the primary forest classes (Classes 1 and 2) were mapped well by all algorithms, while closed shrubland and savanna (Classes 6 and 9) were particularly problematic for the DT and Gaussian ARTMAP algorithms.

3.1.2. *VLC classification system*

Table 4 presents the class names and distribution by size class by VLC class of the STEP training, testing and validation sites. For mapping the VLC classification using Gaussian ARTMAP, parameter values of $\rho = 0.6$ and a variance of 30 were selected to train each of the five train and test iterations based on exploring the relationship of the vigilance parameter to training. This vigilance value is a compromise between using a high vigilance which tends to fit the training data (exemplars) well to the output classes and the need to generalize training data to the output classes. The accuracies for the Gaussian ARTMAP runs are reported in table 5. Both the per-class and overall accuracy were relatively stable for each of the five train–test iterations (range = 80.92–83.86%, SD = 0.945), and the mean overall accuracy for the VLC Gaussian classifications is 82.23%.

The final VLC map for Central America was based on the supervised Gaussian ARTMAP, although as with the IGBP classification test, the Fuzzy ARTMAP and DT algorithms provided similar results. The final VLC map was produced by using all of the train and test site data since the accuracy was already established and it was assumed that this would improve the overall accuracy slightly (figure 2). Spatial filtering was employed using a 3×3 low-pass filter to remove isolated, individual pixels. Filtering improved the overall accuracy of the VLC map by approximately 2%. Area statistics on the distribution of the Central America Vegetation and Land cover classes were then generated (table 5). The largest classes of vegetation and land cover are tropical broadleaf evergreen forest (38%) and agriculture (29%), and the total forested area is estimated to be approximately 54%.

The distribution of the VLC classes coincides with what might be expected based on previous mapping studies, although this study represents the most detailed and comprehensive assessment to date of Central America. The accuracy contingency table of this map is reported in table 6, not as the true independent accuracy assessment (table 5), but to depict the nature of misclassification among classes. Analysis of the classification error rates indicates that while closed forests were generally mapped reliably, open vegetation had a higher error rate. The nature of the classification systems, the vegetation and land cover types and the AVHRR spatial resolution are all problematic, as it is difficult both to define sites and map

Table 2. Regional IGBP Classification results (mean % classification accuracy of 5 runs).

IGBP class	Class name	Train–test pixels	DTC: non-boosted	DTC: boosted	Gaussian ARTMAP	Fuzzy ARTMAP
1	Evergreen needleleaf forest	1515	74.87	88.18	84.49	79.00
2	Evergreen broadleaf forest	3575	84.55	96.15	91.55	79.00
3	Deciduous needleleaf forest					
4	Deciduous broadleaf forest	370	63.82	81.97	75.41	83.90
5	Mixed forest	845	65.55	82.18	72.31	76.90
6	Closed shrublands	125	54.15	58.40	46.40	83.00
7	Open shrublands	335	65.66	83.61	82.69	93.00
8	Woody savannas	470	65.12	82.46	77.66	85.80
9	Savannas	60	34.25	37.58	15.00	78.10
10	Grasslands	845	70.48	85.38	78.22	81.20
11	Permanent wetlands	800	65.92	78.17	72.00	80.60
12	Croplands	1950	70.37	86.96	83.69	68.00
13	Urban and built-up	265	57.25	77.69	71.32	82.90
14	Cropland mosaics	365	68.62	83.42	76.99	91.70
15	Snow/Ice					
16	Barren or sparsely vegetated	35	29.83	81.83	28.57	72.20
17	Water bodies	440	98.48	98.89	97.05	95.40
Total/mean		11 995	74.79	88.16	82.77	79.30

Table 3. Regional IGBP supervised G-ART classification accuracy.

Regional IGBP class	Reference data IGBP class (% 1 km^2 pixel agreement)																	
	1	2	3	4	5	6	7	8	9	10	11	12	13	14	15	16	17	Test pixels
1	**65.35**	11.88			2.64		0.66			5.94	6.27	6.93	0.33					303
2	5.03	**87.13**		0.42	1.40			0.42		0.84	0.70	2.66		1.12			0.28	715
3																		0
4	6.76	16.22		**50.00**	1.35					5.41		17.57		1.35			1.35	74
5	15.38	6.51		1.78	**49.70**		0.59	0.59		9.47	5.33	10.65						169
6	4.00	24.00				**4.00**		4.00		24.00		36.00		4.00				25
7	10.45	1.49					**44.78**	11.94		13.43		16.42					1.49	67
8	10.64	13.83		1.06			1.06	**38.30**		7.45	5.32	21.28	1.06					94
9	8.33	33.33							**0.00**	8.33	16.67	25.00		8.33				12
10	1.18	2.96		1.78	1.78		1.18			**78.11**	0.59	12.43						169
11	15.00	14.38		0.63	1.88		0.63	4.38		3.13	**49.38**	6.88	0.63	0.63			2.50	160
12	8.72	8.21		0.26	1.28					8.46	1.28	**71.28**		0.51				390
13	5.66	5.66			1.89			3.77			7.55	11.32	**64.15**					53
14		38.36		2.74						10.96		6.85	2.74	**38.36**				73
15																		0
16		42.86					14.29			42.86						**0.00**		7
17													2.25	1.12			**96.63**	89
sum																		2400

Table 4. VLC classification system and site distribution.

Class	VLC class name	Sites	Pixels (km^2)	Mean area (km^2)
1	Needleleaf evergreen forest	36	1294	35.94
2	Broadleaf evergreen forest	115	2989	25.99
3	Mixed broadleaf/needleleaf evergreen forest	17	609	35.82
4	Broadleaf deciduous forest	16	355	22.19
5	Swamp forest	12	227	18.92
6	Palm forest	6	229	38.17
7	Mangroves	20	174	8.70
8	Needleleaf evergreen woodland	8	271	33.88
9	Broadleaf evergreen woodland	6	196	32.67
10	Broadleaf deciduous woodland	2	70	35.00
11	Mixed broadleaf/needleleaf woodland	7	208	29.71
12	Broadleaf evergreen savanna	3	112	37.33
13	Needleleaf evergreen savanna	5	386	77.20
14	Broadleaf evergreen scrub/shrub	7	171	24.43
15	Cactus/thorn scrub	5	168	33.60
16	Swamp scrub/shrub	12	293	24.42
17	Perennial graminoid grassland	15	371	24.73
18	Herbaceous wetland	7	93	13.29
19	Barren rock, sand, and soil	3	33	11.00
20	Marine	12	914	76.17
21	Limnic	9	316	35.11
22	Disturbed forest complex	4	107	26.75
23	Mixed urban/vegetation complex	7	241	34.43
24	Agriculture	75	2930	39.07
25	Urban/industrial	19	244	12.94
	Mean	428	13 001	30.38

small and linear patch vegetation such as riparian and mangrove forests. The size of the train and test samples did not necessarily influence accuracy. Regression analysis of sample size on accuracy resulted in an r^2 of 0.52, which is most likely skewed based on the several large classes with high accuracy (agriculture and broadleaf evergreen forest). While the deciduous and mixed woodland classes were undersampled and had poor accuracy, evergreen woodland and urban/industrial classes were both small but of high accuracy.

3.2. *Comparative analyses*

Two comparative analyses were performed to evaluate the relative accuracy and performance of the classification systems and approaches. These comprised comparison of this study's supervised regional and the existing global IGBP maps, and this study's derived VLC map with an existing ecoregion map.

3.2.1. *Regional and global IGBP classifications*

A global map of the IGBP using the same AVHRR NDVI data used in this study had previously been produced and distributed by the USGS-EROS Data Center (Belward and Loveland 1995). This 1 km IGBP classification, derived using unsupervised classification, was the subset for the study area from the global map for use in a comparative analysis of land cover distribution. Contingency table analysis of this study's supervised regional and the existing unsupervised global

Table 5. VLC G-ART accuracy and areal estimates.

Class	Vegetation and landcover type	Test pixels (1 km^2)	Mean accuracy (% pixel agreement)	Area estimate (km^2)	% area estimate
1	Tropical needleleaf evergreen forest	205	81.07	46 345	7.49
2	Tropical broadleaf evergreen forest	637	91.02	234 911	37.95
3	Tropical broadleaf/needleleaf evergreen forest	139	71.22	12 139	1.96
4	Tropical broadleaf deciduous forest	71	63.94	22 713	3.67
5	Tropical swamp forest	43	46.98	11 228	1.81
6	Palm forest	45	84.44	2477	0.40
7	Mangroves	34	24.71	4721	0.76
8	Tropical needleleaf evergreen woodland	42	68.57	3436	0.56
9	Tropical broadleaf evergreen woodland	40	81.50	7756	1.25
10	Tropical broadleaf deciduous woodland	14	92.86	1782	0.29
11	Tropical broadleaf/needleleaf woodland	20	76.00	2531	0.41
12	Tropical broadleaf evergreen savanna	15	84.00	1044	0.17
13	Tropical needleleaf evergreen savanna	85	93.18	7190	1.16
14	Tropical broadleaf evergreen scrub/shrub	35	73.14	5081	0.82
15	Tropical cactus/thorn scrub	34	79.41	3379	0.55
16	Tropical swamp scrub/shrub	47	59.15	12 366	2.00
17	Tropical perennial graminoid grassland	74	62.70	20 589	3.33
18	Tropical herbaceous wetland	29	51.72	5082	0.82
19	Barren rock, sand, and soil	10	26.00	316	0.05
20	Marine	48	100.00	1854	0.30
21	Inland water (limnic)	81	96.54	13 655	2.21
22	Forest-woodland-agriculture complex	22	34.55	12 977	2.10
23	Urban/vegetation complex	49	74.69	4669	0.75
24	Agriculture	585	89.40	179 730	29.03
25	Urban/industrial	49	83.67	1077	0.17
Total		2453	82.23	619 048	100.00

classification maps indicated a disparity of agreement in cover classes both in regional estimates and spatial agreement (table 7). The wetland and closed shrub categories of both the global unsupervised and regional supervised IGBP are especially problematic in terms of accuracy based on the site database, though it is to be expected that the overall accuracy of the regional classification would be better, given the different levels of mapping intensity. The global IGBP map is also a preliminary map which is currently undergoing revision and validation. Both IGBP classification systems compared well for closed forests, especially evergreen broadleaf forest which is the dominant forest cover type of the region. The IGBP agreement was poorest for savannas (Class 9), and for the barren/sparsely vegetated class (Class 16). This may largely be due to the small sampling size of these classes.

The area estimates of the global and regional IGBP land cover are generally in agreement (table 6). These two maps are not in agreement locationally however. The

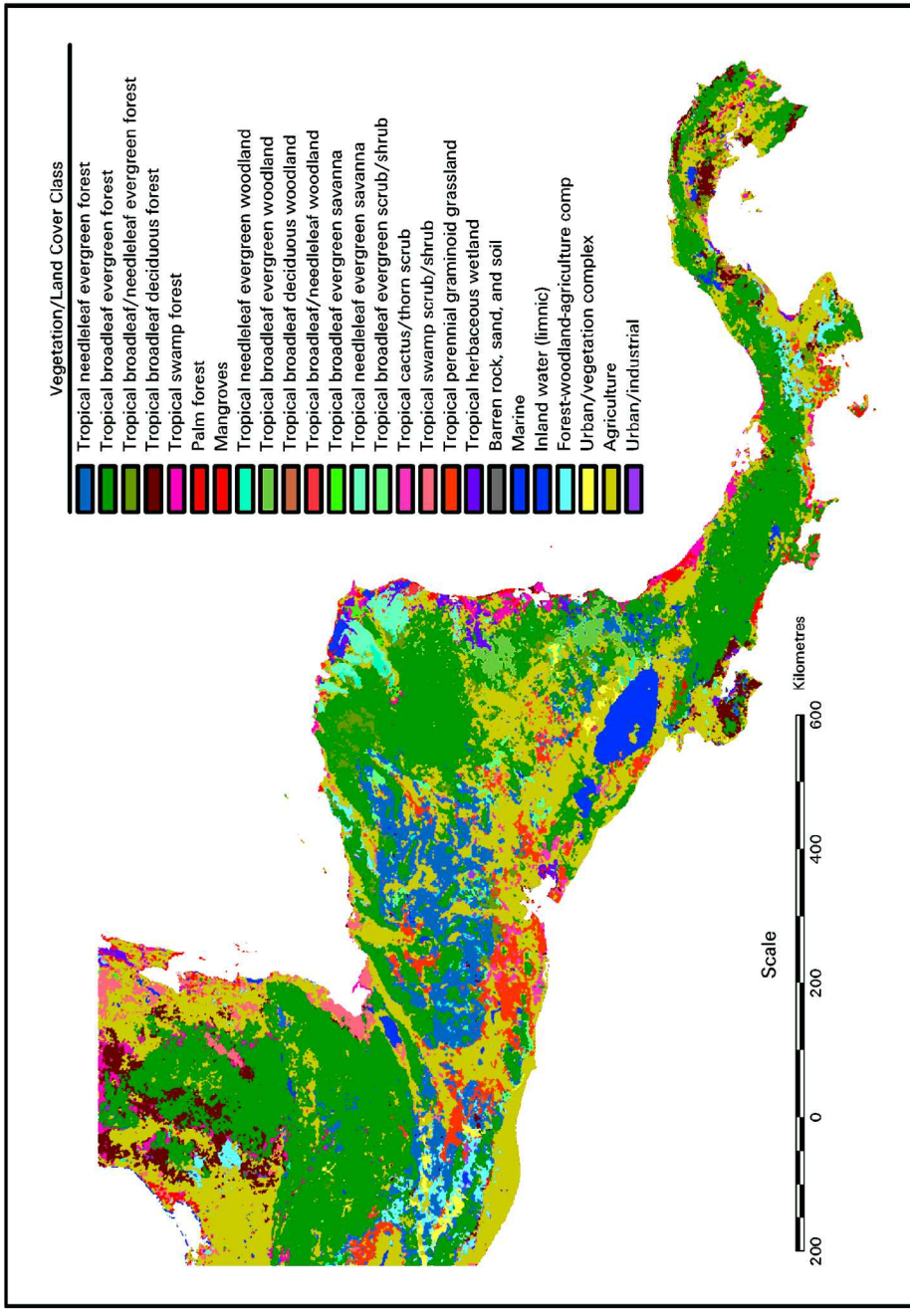

Figure 2. VLC map.

Table 6. VLC supervised G-ART classification accuracy.

	Reference data class (dn's = 1 km^2)																										
Class	1	2	3	4	5	6	7	8	9	10	11	12	13	14	15	16	17	18	19	20	21	22	23	24	25	Test pixels	% correct
1	**78.54**	6.83	0.98	0.49									1.46			0.98	0.49							10.24		205	
2	1.26	**93.25**	0.78	0.16	0.47			0.47		0.16				0.16		0.16					0.16		0.31	2.35	0.31	637	93.25
3	5.04	7.19	**73.33**				0.72						0.72				0.72							12.23		139	73.38
4	1.41	5.63		**70.42**										1.41		1.41	7.04							12.68		71	70.42
5	2.33	13.95			**55.81**											2.33					4.63			20.93		43	55.81
6	2.22	6.67		2.22		**75.56**																		13.33		45	75.56
7	17.65	5.88	5.88	2.94			**32.35**					8.82				2.94	5.88							8.82	8.82	34	31.43
8	2.38	2.38						**80.95**					2.38			2.38								9.52		42	80.95
9	2.50	5.00							**75.00**					5.00								2.50		10.00		40	75.00
10										**100**																14	100.00
11											**90.00**					5.00	5.00									20	90.00
12												**100**														15	100.00
13		1.18											**95.29**					1.18				1.18		1.18		85	95.29
14	2.86				2.86								11.43	**77.14**				2.86						2.86		35	77.14
15				2.94											**85.29**									11.76		34	85.29
16	4.26	6.38			6.38								8.51			**57.45**								17.02		47	57.45
17	1.35	5.41			1.35										6.76		**66.22**							18.92		74	66.62
18													41.38					**41.38**						17.24		29	41.38
19		10.00	10.00								10.00								**30.00**					40.00		10	30.00
20																				**100**						48	100.00
21																		1.23			**96.30**		1.23		1.23	81	96.30
22	9.09	9.09						4.55					18.18		9.09							**40.91**		9.09		22	40.91
23		4.08						2.04		4.08			2.04	2.04									**75.51**	6.12	4.08	49	75.51
24	2.56	2.56	1.20	0.17	0.17		0.17	0.17					0.17		0.51	1.03	0.34	0.17	0.17		0.17			**89.91**	0.51	585	90.07
25	2.04		2.04					2.04																4.03	**89.80**	49	89.80

Table 7. Regional and global classification agreement.

Regional IGBP class	Global IGBP class (% pixel agreement)																	
	1	2	3	4	5	6	7	8	9	10	11	12	13	14	15	16	17	Pixel sum
1	**14.15**	39.22			6.67				2.70	0.18	0.01	36.10	0.08	0.88				60 081
2	6.60	**63.07**			4.10		0.15	2.54	0.39	4.01	0.06	18.23	0.02	0.81		0.01		260 015
3																		0
4	20.70	7.47		**0.00**	21.16	0.01		0.10	6.92	0.02		42.99	0.11	0.53				11 947
5	5.41	62.33			**7.70**	0.01	0.04		2.16	0.54	0.48	20.49	0.02	0.81				27 283
6	1.71	18.63			38.57	**0.00**		0.70		0.10		38.77		1.51				993
7	8.43	6.03		0.15	7.61	0.35	**0.00**	6.22	2.37			66.90	0.11	1.84				9967
8	30.46	14.32			10.32	0.01		**0.06**	0.46	0.06	0.53	42.00	0.14	1.65				12 382
9	8.63	8.99			2.88	1.44			**1.08**	1.80		38.13		37.05				278
10	4.23	22.42		0.01	7.69			23.50	1.20	**3.08**		36.49	0.14	1.23				50 046
11	12.43	21.79			12.90	0.01	0.40		8.24	0.12	**0.93**	38.65	0.14	4.38				30 831
12	9.37	24.23		0.03	8.21	0.01		10.98	0.78	0.72		**45.20**	0.12	0.36				124 728
13	28.10	0.36			0.79	0.63	2.35	1.06	5.91	11.04	8.42	35.57	**4.04**	1.74				4431
14	10.20	33.73			17.54			0.73	1.42	0.94		34.81	0.18	**0.45**				10 136
15																		0
16							41.67					41.67			8.33	**8.33**		12
17													0.04				**99.96**	18 457

kappa coefficient, used as a pair-wise indicator of agreement where random agreement is discounted (Congalton *et al.* 1983, Congalton 1991), suggests that the estimates of land cover are significantly different at the 95% confidence level. Because the same data and classification systems were used, these results indicate that area estimates of land cover are a function of the classification model used to ascribe site data to the regional landscape using remote sensing data.

3.2.2. *Ecoregional analyses*

Ecoregional classification systems are defined based on a number of criteria. Some of these approach landscape classification systems (e.g. Omernik 1987) while others are more bioregional (e.g. Dinerstein *et al.* 1995). The most prominent ecoregional systems are those of Bailey (1980) and Omernik (1987), although neither system has been applied in any detail to Central America. A terrestrial ecoregion map for Latin America was compiled from existing maps and expert opinion by The World Bank and World Wildlife Fund (WB/WWF) (Dinerstein *et al.* 1995). The WB/WWF classification system is based on a three-level hierarchy of ecosystem type, habitat type and ecoregion. At the top level, five Major Ecosystem Types are defined primarily on the minimal area that is relevant to ecological processes and conservation management, response characteristics to major disturbance, and similar levels of beta diversity within types, defined as the rate of turnover of species along environmental gradients. The Major Ecosystem Types are tropical broadleaf forests, conifer/temperate broadleaf forests, grasslands/savannas/shrublands, xeric formations, and mangroves.

At the second level, eleven habitat types are based on structure, climate regime, ecological processes, and a beta diversity species turnover-to-distance criterion. At the third (finest) level, ecoregions are defined as units of geographically discrete habitat types or assemblages of natural communities that share a majority of their species, ecological dynamics, and environmental conditions that can be mosaics of specific, individual habitat types (Dinerstein *et al.* 1995). The distribution of the 24 WB/WWF Ecoregions found within the study area is summarized in table 8.

The WB/WWF ecoregions provide a useful context for relating the historical distribution of ecoregions within Central America to their current distribution as determined in this study. The distribution of VLC classes within WB/WWF ecoregions was calculated based on the intersection of the two maps in raster format at 1 km spatial resolution. Table 9 is a class-by-class assessment of the distribution of IGBP classes within the WB/WWF ecoregions. The important considerations are that while the WB/WWF ecoregions represent potential or historical distributions of a set of ecoregions, the VLC classification map provides a remote sensing based depiction of the actual landscape. The analysis of the distribution of the VLC classes in relation to the WB/WWF ecoregions indicates that there is generally agreement on where vegetation and land cover types are located within ecoregions, that is, VLC maps pine forests within pine forest ecosystems.

A significant finding of this study is the distribution of modified types within ecoregions. At least 31% of the landscape of Central America is anthropogenic in nature, while the percentage of anthropogenic types within specific classes is variable and class-specific. The estimate of the remaining forest within the Dry Forest Ecoregion is only 16%. Some 59% of the Belizean Swamp Forest and 57% of the Belizean Pine Forest Ecoregions are considered to be agricultural lands. The analysis indicates that 33% of the Choco-Darien Forests of Panama is in agriculture, while

Table 8. WB/WWF ecoregion classification and distribution.

Class	Ecoregion	Area (km^2)	% Area
5	Mangrove	4556	0.77
8	Tehuantepec moist forests	99 372	16.76
9	Yucatan moist forests	46 308	7.81
10	Sierra Madre moist forests	6419	1.08
11	Central American montane forests	7726	1.30
12	Belizean swamp forests	4230	0.71
13	Central American Atlantic moist forests	156 879	26.46
14	Costa Rican seasonal moist forests	10 567	1.78
15	Isthmian-Pacific moist forests	28 480	4.80
16	Talamancan montane forests	16 301	2.75
39	Choco-Darien moist forests	13 477	2.27
40	Eastern Panamanian montane forests	2276	0.38
68	Balsas dry forests	3315	0.56
71	Yucatan dry forests	1074	0.18
72	Central American Pacific dry forests	46 580	7.86
73	Panamanian dry forests	5088	0.86
102	Central American pine-oak forests	113 984	19.22
103	Belizean pine forests	2821	0.48
104	Miskito pine forests	15 508	2.62
108	Tabasco/Veracruz savannas	3278	0.55
109	Tehuantepec savannas	1227	0.21
126	Veracruz palm savannas	120	0.02
127	Quintano Roo wetlands	917	0.15
136	Costa Rican paramo	30	0.01
166	Motagua Valley thornscrub	2394	0.40
Total		592 927	100.00

some 59% is forested. The distribution of actual vegetation and land cover within the WB/WWF ecoregions underlines the importance of remote sensing based mapping to quantify the current status of the landscape, providing quantitative descriptions of the patterns of human modification of the landscape.

4. Conclusions

This research has demonstrated the feasibility of rapidly generating regional test sites from high resolution satellite data, ancillary information and expert knowledge. These site data can be applied to moderate resolution, regional satellite data to map multiple land cover and vegetation classifications with good statistical results. The research indicates that map accuracy is a function of the classification system and categories, as well as the input data. Estimates of land cover are equally a function of both the source data used to derive them and the classification model used to ascribe site data to the regional landscape using remote sensing data. The analysis demonstrates that mapping at regional scales is feasible, with classification accuracy associated with the map estimated at upwards of 85%. Applying the IGBP classification system, the DT averaged almost 88%, Gaussian ART almost 83%, and Fuzzy ART NN 79%. Comparison with existing ecoregion maps indicates that using remote sensing data provides a much more realistic assessment of the true nature of the distribution of vegetation and land cover.

Research in testing the NN and DT algorithms is ongoing. A significant hurdle is the development of the global site network needed to train, test and validate global

Table 9. Relationship of VLC and WB/WWF ecoregions.

VLC class	WB/WWF Ecoregion (per cent pixel agreement)																											Pixels (1 km^2)
	2	3	4	5	6	8	9	10	11	12	13	14	15	16	39	40	68	71	72	73	102	103	104	108	109	127	136	166	
1						3.45	0.43	0.98	3.72	0.01	16.84	1.20					0.99	0.02	1.87	0.02	69.07	0.46	0.01		0.04			0.91	46 263
2	0.01		0.01			29.02	4.95	0.60	1.55	0.12	33.39	2.07	5.19	6.67	2.36	0.66	0.33	0.08	2.28	0.07	9.26	0.14	1.03		0.15		0.01	0.07	232 960
3	0.06		0.01	0.59	0.07	2.26	0.08	0.33	0.60	0.02	52.14	2.19	8.82	2.16	3.46	0.31			3.90	0.28	16.36	0.05	6.17					0.15	12 116
4	0.09	0.05	0.28	0.24		20.36	38.03	0.54	0.11	0.61	10.58	8.18	3.38	0.04	6.01	2.14	0.02	2.08	4.52	0.92	1.68	0.10	0.04						22 160
5				0.72	0.13	21.60	31.70			0.84	26.34	0.01	3.45		5.38	0.01		3.16	0.22		0.01	0.06	6.21	0.01		0.15			8934
6				0.86			1.16	5.55		1.21	42.71	2.07	36.51	5.60	2.92	0.10			0.25			0.25	0.81						1983
7	0.15	0.11	2.18	2.06	3.09	4.35	44.69			4.93	7.60		17.27	0.04	1.11		0.38		1.72	0.46		1.68	2.18	0.23		5.77			2618
8	0.47					1.89	3.32	0.44	1.54		16.42	0.49	2.18		0.41	0.03	0.44		6.93	0.47	33.77		31.15		0.06				3435
9									0.28		91.97		0.12	0.04					2.10		1.10		4.39						7750
10				0.39				4.13	5.61		10.92	0.82	9.24		0.51		0.62		6.12	7.10	52.51		2.03						2565
11	0.31		0.04	0.35		7.65	0.66	0.27		1.64	37.49	0.66	1.06		0.88		2.70		14.72		15.87	1.59	14.10						2262
12		1.08		0.43		0.54	13.77			2.06	48.81				25.16				2.28			0.43	5.31			0.11			922
13	0.11		0.55			1.23	0.43	0.40		1.04	12.45	0.16	0.51						3.81	0.02	0.21	1.33	76.96			0.81			6329
14						0.37		2.05	1.55		30.29	1.89	0.93		0.18				10.14		52.57							0.04	5081
0		1.50	1.41	0.78		0.51	0.96		0.06		3.53	0.15			0.84			0.06	69.13	0.36	18.73							2.00	3343
16	0.05	0.05	0.09	1.11	0.07	24.70	27.64			7.58	18.03	0.46	3.65		2.76	0.23	0.14		1.82	0.52	5.98	3.96	0.23		0.03	0.72		0.17	11 074
17		0.02	0.06	0.06	0.04	0.44	1.02	1.23	0.42	0.56	5.52	0.69	4.74	0.09	0.89	0.10	1.24		20.60	0.43	59.45	0.15	0.23		1.14	0.07		0.82	20 241
18	2.08	0.03	12.43	4.11		0.18	4.40	0.62		0.32	10.73	1.96	0.26						8.04	2.35		0.47	37.92			14.11			3410
19											12.66		17.41	37.97	12.34	19.62													316
20	1.22			14.98		17.43	15.90			0.92	43.43				0.61					0.31		0.31	3.36	1.53					327
21	0.06					7.56	1.46		0.58	0.74	42.34	3.03	7.64		6.01		0.11		9.08	0.03	16.03		1.32	1.35	2.65				3625
22						8.47	4.41	8.43	5.84		9.34	0.02	25.62	0.09	0.93	0.03	0.40		0.88	2.39	33.10				0.06				12 911
23	0.09					4.08			16.07		10.15	2.75	0.15	0.73		0.04	0.04		19.91	0.99	44.54		0.47						4661
24	0.12	0.47	0.37	0.52	0.05	10.56	10.06	1.47	0.18	1.41	23.05	1.35	4.25	0.12	2.49	0.03	0.94	0.07	16.29	2.21	18.00	0.91	2.05	1.81	0.27	0.07		0.88	174 574
25			0.09					7.18	7.74		3.26	2.24		0.28					23.02		55.36				0.47			0.37	1073

land cover maps and biophysical parameters. Continuing efforts to develop a global database of sites using the STEP model have been expanded to North America. Given the positive results of testing this methodology regionally using AVHRR data, significant improvements using MODIS data can be expected considering the improved spectral and radiometeric resolution and locational accuracy of the MODIS system.

Acknowledgments

This research was supported by the Proyecto Ambiental Regional de Centroamerica–Central American Protected Area System (PROARCA–CAPAS) and the Comision de la Centroamericana de Ambiente y Desarrollo (CCAD), the International Resources Group, Ltd (IRG), The Nature Conservancy, the US Agency for International Development (USAID) and NASA (Contract NAS5-31369).

The authors also wish to acknowledge the Central America Vegetation Working Group; Xiaojun Li and Roger Sayre of The Nature Conservancy; Bennett Sandler of the Center for Conservation Biology-Stanford University; Tom Loveland, Brad Reed, Jess Brown and Jeff Eidenshink of USGS-EDC; Jose Courrau of PROARCA–CAPAS; Nathan Morrow and Curtis Woodcock of the Center for Remote Sensing/ Department of Geography, Boston University; and Jim Williamson of the Department of Cognitive and Neural Systems, Boston University, for their support.

References

Achard, F., and Estreguil, C., 1995, Forest classification of Southeast Asia using NOAA AVHRR data. *Remote Sensing of Environment*, **54**, 198–208.

Bailey, R. G., 1980, Description of the Ecoregions of the United States. Misc. Publ. 1391, USDA, Washington DC, USA.

Belward, A., and Loveland, T. R., 1995, The IGBP 1km Land Cover Project. *Proceedings of the 21st Annual Conference of the Remote Sensing Society, Southampton, UK, 11–14 September, Nottingham, Remote Sensing Society*, 1099–1106.

Bonan, G. B., 1996, A land surface model (LSM version 1.0) for ecological, hydrological, and atmospheric studies: technical description and user's guide. NCAR/TN-417+STR, NCAR Technical Note, National Center for Atmospheric Research, Boulder, CO, USA.

Brodley, C. E., 1995, Recursive automatic bias selection for classifier construction. *Machine Learning*, **20**, 63–94.

Brodley, C. E., and Utgoff, P. E., 1995, Multivariate decision trees. *Machine Learning*, **19**, 45–77.

Carpenter, G. A., Grossberg, S., Markuzon, N., Reynolds, J. H., and Rosen, D. B., 1992, Fuzzy ART: a neural network architecture for incremental supervised learning of analog multidimensional maps. *IEEE Transactions on Neural Networks*, **3**, 698–713.

Carpenter, G. A., Grossberg, S., and Reynolds, J. H., 1991a, ARTMAP: supervised real-time learning and classification of nonstationary data by a self-organizing neural network. *Neural Networks*, **4**, 566–588.

Carpenter, G. A., Grossberg, S., and Rosen, D. B., 1991b, Fuzzy ART: fast stable learning and categorization of analog patterns by an adaptive resonance system. *Neural Networks*, **4**, 759–771.

Cihlar, J., 1996, Identification of contaminated pixels in AVHRR composite images for studies of land biosphere. *Remote Sensing of Environment*, **56**, 149–163.

Congalton, R. G., 1991, A review of assessing the accuracy of classifications of remotely sensed data. *Remote Sensing of Environment*, **7**, 33–46.

Congalton, R. G., Oderwald, R. G., and Mead, R. A., 1983, Assessing Landsat classification accuracy using discrete multivariate analysis statistical techniques. *Photogrammetric Engineering and Remote Sensing*, **49**, 1671–1678.

DeFries, R. S., and Townshend, J. R. G., 1994, NDVI-derived land cover classifications at a global scale. *International Journal of Remote Sensing*, **15**, 3567–3586.

Dickinson, R. E., Henderson-Sellers, A., and Kennedy, P. J., 1993, *Biosphere Atmosphere Transfer Scheme (BATS) Version l as coupled to the NCAR Community Climate Model*. NCAR Technical Note 387, Boulder: NCAR, 80 pp.

Diego Gomez, L., 1985, *Mesoamerica Vegetation Map 1. Provisional vegetation types map of Mexico and Central America* (Washington, D. C.: The Nature Conservancy).

Dinerstein, E., Olson, D. M., Graham, D. J., Webster, A. L., Primm, S. A., Bookbinder, M. P., and Ledec, G., 1995, *A Conservation Assessment of the Terrestrial Ecoregions of Latin America and the Caribbean* (Washington, D.C.: The World Bank).

Duggin, M. J., Piwinski, D., Whitehead, V., and Ryland, G., 1982, Scan-angle dependence of radiance recorded by the NOAA-AVHRR. *Proceedings SPIE*, **363**, 98–101.

Eidenshink, J. C., and Faundeen, J. L., 1994, The 1-km AVHRR global land data set: first stages in implementation. *International Journal of Remote Sensing*, **15**, 3443–3462.

Friedl, M. A., and Brodley, C. E., 1997, Decision tree classification of landcover from remotely sensed data. *Remote Sensing of Environment*, **61**, 399–409.

Friedl, M. A., Brodley, C. E., and Strahler, A. H., 1999, Maximizing land cover classification accuracies produced by decision trees at continental to global scales. *IEEE Transactions on Geoscience and Remote Sensing*, **37**, 969–977.

Gopal, S., Sklarew, D. M., and Lambin, E., 1994, Fuzzy-neural networks in multitemporal classification of landcover change in the Sahel. *New Tools for Spatial Analysis, Proceedings of the Workshop, Lisbon, 18–20 November 1993* (Luxembourg: Office for Official Publ. Eur. Communities), pp. 69–81.

Gopal, S., Woodcock, C., and Strahler, A. H., 1999, Fuzzy ARTMAP classification of global land cover from the 1 degree AVHRR data set. *Remote Sensing of Environment*, **67**, 230–243.

Henderson-Sellers, A., 1987, Effects of change in land use on climate in the humid tropics. In *The Geophysiology of Amazonia: Vegetation and Climate Interactions*, edited by R. E. Dickinson (New York: Wiley), pp. 463–493

Holben, B., 1986, Characteristics of maximum-value composite images from multitemporal AVHRR data. *International Journal of Remote Sensing*, **7**, 1417–1434.

Holdridge, L. R., 1962a, *Mapa ecologico de Honduras* (Washington, D. C.: Organization of American States).

Holdridge, L. R., 1962b, *Mapa ecologico de Nicaragua* (Managua, Nicaragua: United States Agency for International Development).

Holdridge, L. R., 1967, *Life Zone Ecology* (San Jose, Costa Rica: Tropical Science Center).

Holdridge, L. R., 1975a, *Zonas de vidas ecologicas de El Salvador; Proyecto Desarrollo, Forestal y Ordenacion de Cuencas Hidrograficas* (New York: Food and Agriculture Organization).

Holdridge, L. R., 1975b, *Mapa ecologico de El Salvador* (San Salvador: Ministerio de Agricultura y Ganaderia).

Justice, C., Vermote, E., Townshend, J., *et al*., 1998, The Moderate Resolution Imaging Spectroradiometer (MODIS): land remote sensing for global change research. *IEEE Transactions on Geoscience and Remote Sensing*, **36**, 1228–1249.

Lippmann, R. P., 1989, Pattern classification using neural networks. *IEEE Communications Magazine*, **27**, 47–55.

Loveland, T. R., Merchant, J. W., Brown, J. F., Ohlen, D. O., Reed, B. C., Olson, P., and Hutchinson, J., 1995, Seasonal land-cover of the United States. *Annals Association of American Geographers*, **85**, 339–355.

Loveland, T. R., Merchant, J. W., Ohlen, D. O., and Brown, J. F., 1991, Development of a land-cover characteristics database for the conterminous U. S. *Photogrammetric Engineering and Remote Sensing*, **57**, 1453–1463.

Malingreau, J.-P., 1986, Global vegetation dynamics: satellite observation over Asia. *International Journal of Remote Sensing*, **7**, 1121–46.

Matthews, E., 1983, Global vegetation and land-use: new-high resolution data bases for climate studies. *Journal of Climate and Applied Meteorology*, **22**, 474–487.

Muchoney, D. M., Grossman, D. H., and Solomon, R., 1991, Rapid ecological assessment

for conservation planning. *ASPRS/ACSM Technical Papers* (Bethesda, MD: ASPRS), pp. 141–145.

Muchoney, D. M., Strahler, A., Hodges, J., and Locastro, J., 1999. The IGBP DISCover confidence sites and the system for terrestrial ecosystem parameterization: tools for validating global land cover data. *Photogrammetric Engineering and Remote Sensing*, **65**, 1061–1067.

Myneni, R. B., Nemani, R., and Running, S. W., 1997, Estimation of global leaf area index and absorbed PAR using Radiative Transfer Models *IEEE Transactions on Geoscience and Remote Sensing*, **35**, 1380–1393.

Nemani, R., and Running, S. W., 1996, Implementing a hierarchical global vegetation classification in ecosystem function models. *Journal of Vegetation Science*, **7**, 337–346.

Nemani, R., and Running, S. W., 1997, Land cover characterization using multitemporal red, near-IR, and thermal-IR data from NOAA/AVHRR. *Ecological Applications*, **7**, 79–90.

Olson, J. S., and Watts, J., 1982, Major world ecosystem complexes. Earth's Vegetation and Atmospheric Carbon Dioxide. In *Carbon Dioxide Review*, edited by D. B. Jones (Oxford: Oxford University Press), pp. 388–99.

Olson, J. S., Watts, J., and Allison, L., 1983, Carbon in Live Vegetation of Major World Ecosystems. Report W-7405-ENG-26U.S. Dept. of Energy, Oak Ridge National Lab., Oak Ridge, TN, USA.

Omernik, J. M., 1987, Ecoregions of the conterminous United States. *Annals Association of American Geographers*, **77**, 118–125.

Quinlan, J. R., 1993, *C4.5: Programs for Machine Learning* (San Mateo, CA: Morgan Kaufmann).

Quinlan, J. R., 1996, Bagging, boosting, and C4.5. *Proceedings of the 13th National Conference on Artificial Intelligence*, (Portland, OR: AAAI Press), pp. 725–730.

Running, S. W., Loveland, T. R., and Pierce, L. L., 1994, A vegetation classification logic based on remote sensing for use in global biogeochemical models. *Ambio*, **23**, 77–81.

Running, S. W., Loveland, T. R., Pierce, L. L., Nemani, R., and Hunt, E. R. Jr., 1995, A remote sensing based vegetation classification logic for global land cover analysis. *Remote Sensing of Environment*, **51**, 39–48.

Sellers, P. J., Mintz, Y., Sud, Y. C., and Dalcher, A., 1986, A simple biosphere model (SiB) for use within general circulation models. *Journal of Atmospheric Science*, **43**, 503–531.

Sellers, P. J., Randall, D. A., Collatz, G. J., *et al*., 1996, A revised land surface parameterization (SiB2) for atmospheric GCMs. Part 1: model formulation. *Journal of Climate*, **9**, 676–705.

Sellers, P. J., Shuttleworth, W. J., Dorman, J. L., Dalcher, A., and Roberts, J. M., 1989, Calibrating the Simple Biosphere Model for Amazonia tropical forest using field and remote sensing data. Part I: Average calibration with field data. *Journal of Applied Meteorology*, **28**, 727–759.

Shapire, R. E., 1990, The strength of weak learnability. *Machine Learning*, **5**, 197–227.

Stone, T. A., Schlesinger, P., Houghton, R. A., and Woodwell, G. M., 1994, A map of the vegetation of South America Based on satellite imagery. *Photogrammetric Engineering and Remote Sensing*, **60**, 541–551.

Strahler, A. H., 1980, The use of prior probabilities in maximum likelihood classification of remotely sensed data. *Remote Sensing of Environment*, **10**, 135–163.

Strahler, A., Townshend, J., Muchoney, D., Borak, J., Friedl, M., Gopal, S., Hyman, A., Moody, A., and Lambin, E., 1996, MODIS Land Cover and Land-Cover Change Algorithm Theoretical Basis Document (ATBD), Version 4.1 (Boston: Boston University).

Townshend, J. R. G., Justice, C. O., and Kalb, V. T., 1987, Characterization and classification of South American land cover types using satellite data. *International Journal of Remote Sensing*, **8**, 1189–1207.

Tucker, C. J., Townshend, J. R. G., and Goff, T. E., 1985, African land-cover classification using satellite data. *Science*, **227**, (4685), 369–375.

Van Dijk, A., Calhs, S. I., Sakamoto, C. M., and Decker, W. I., 1987, Smoothing vegetation index profiles: an alternative method for reducing radiometric disturbance in NOAA/AVHRR Data. *Photogrammetric Engineering and Remote Sensing*, **53**, 1059–1067.

WILLIAMSON, J. R., 1995, Gaussian ARTMAP: A neural network for fast incremental learning of noisy multidimensional maps. Technical Report CAS/CNS-95-003, Boston University, USA.

WILSON, M., and HENDERSON-SELLERS, A., 1985, A global archive of land cover and soils data for use in general circulation climate models. *Journal of Climatology*, **5**, 119–143.

ZHU, Z.-L., and YANG, L., 1996, Characteristics of the 1-km AVHRR data set for North America. *International Journal of Remote Sensing*, **17**, 1915–1924.